Continental Shelf Research 232 (2022) 104630

Contents lists available at ScienceDirect

Continental Shelf Research

journal homepage: www.elsevier.com/locate/csr

On group velocity and spatial damping of diurnal continental shelf waves

Jan Erik H. Weber [a,*], Eli Børve [a,b]

[a] Department of Geosciences, University of Oslo, Norway
[b] Akvaplan-Niva AS, Fram Centre, Tromsø, Norway

ARTICLE INFO

Keywords:
Continental shelf waves
Diurnal tidal forcing
Inner porous shelf
Group velocity
Wave damping

ABSTRACT

Diurnal continental shelf waves (CSWs) are studied theoretically for an idealized shelf topography. Wave attenuation is caused by the exchange of fluid on the sloping shelf with an inner region through a permeable coastline. As an example, we consider the region outside Lofoten-Vesterålen in north Norway. Here CSWs with diurnal tidal frequencies are possible in a small wave number range centered around zero group velocity. A previous investigation with a Robin condition (a weighted combination of Dirichlet and Neumann conditions) at the permeable boundary has shown that the spatial damping coefficient becomes infinitely large when the group velocity of the CSWs approaches zero. Here we demonstrate that this is not a result of the mathematical formulation, but reflects a physical reality. We show this by modelling the highly convoluted inner archipelagic region as a series of densely packed vertical Hele Shaw cells. By comparing the two ways of describing a permeable coastal boundary (Robin/Hele Shaw), we may express the Robin parameter in terms of the physical parameters (permeability, eddy viscosity) that characterize the flow on the inner porous shelf. The radiation stresses that drive the Lagrangian mean currents are the same in the two cases. This means that the spatial mean current distribution over the sloping shelf becomes unaltered when we compare the Robin case and the porous inner shelf case.

1. Introduction

It is well known that oscillating fluxes through straits may generate continental shelf waves (CSWs); see e.g. Buchwald and Kachoyan (1987), Middleton (1988), Morrow et al. (1990) for the generation of CSWs along the Australian shelf from oscillating motion in the Bass Strait. In addition, at the south coast of British Columbia, Foreman and Thomson (1997) demonstrate that CSWs are generated when the strong diurnal tidal currents in Juan de Fuca Strait encounter the abrupt topography near the entrance to the strait. Even in cases without a strait, CSWs with diurnal tidal frequency may be generated on the shelf slope if the local group velocity is close to zero due to changes in topography as demonstrated by Cartwright (1969) for the shelf near St. Kilda in the and Lam (1999) for the Greenland shelf.

In north Norway, the strong tidal Moskstraumen is a clear parallel to the oscillating fluxes in the Australian Bass strait, pressing water back and forth across the depth contours of the shelf outside Lofoten. Numerical modelling of the tidal motion in the Lofoten -Vesterålen region reveals a distinct amplification of the currents for the tidal diurnal K_1 component (Ommundsen and Gjevik, 2000; Moe et al., 2002; Børve et al., 2021). In Fig. 1, we have inserted a map of the Lofoten-Vesterålen region.

In Weber and Børve (2021), CSWs were studied at three different locations outside Vesterålen; see Fig. 2. In each transect the shelf geometry was idealized in the same way as in Buchwald and Adams (1968).

The topography at the three transects were very similar, and the dispersion diagrams, using the analysis in Drivdal et al. (2016), are depicted in Fig. 3.

We note from Fig. 3 that CSWs with diurnal frequencies are possible outside Vesterålen in a wave number region centered around zero group velocity.

Usually, in modelling CSWs, the coastline is taken to be a solid wall. However, along the Norwegian coast there are a myriad of small islands and narrow fjords with a lateral scale much smaller than the CSW wavelength, as is evident from Fig. 1. Hence, since CSWs have a velocity component normal to the depth contours, which usually follows the coastline, there will be an exchange of fluid between the CSW and the narrow fjords. In the fjord system, the dissipation will be considerable. This will remove energy from the CSW, and lead to spatial damping as it

* Corresponding author.
E-mail addresses: j.e.weber@geo.uio.no (J.E.H. Weber), elb@akvaplan.niva.no (E. Børve).

https://doi.org/10.1016/j.csr.2021.104630
Received 9 August 2021; Received in revised form 9 November 2021; Accepted 28 November 2021
Available online 7 December 2021

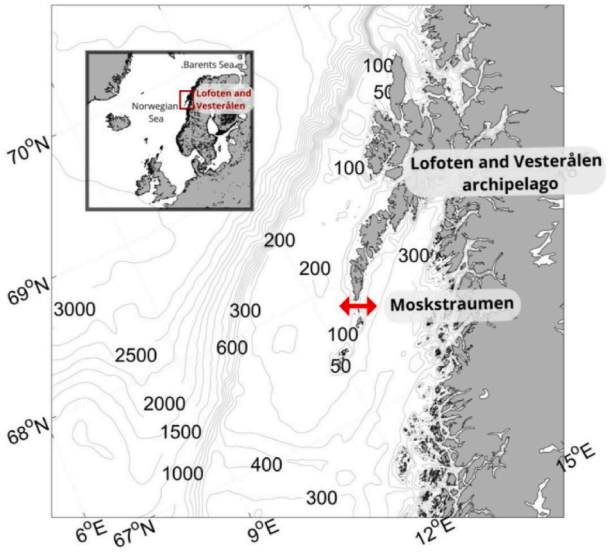

Fig. 1. Map of the Lofoten-Vesterålen region with the depth of the bottom contours in meters. The red arrow indicates the position of Moskstraumen.

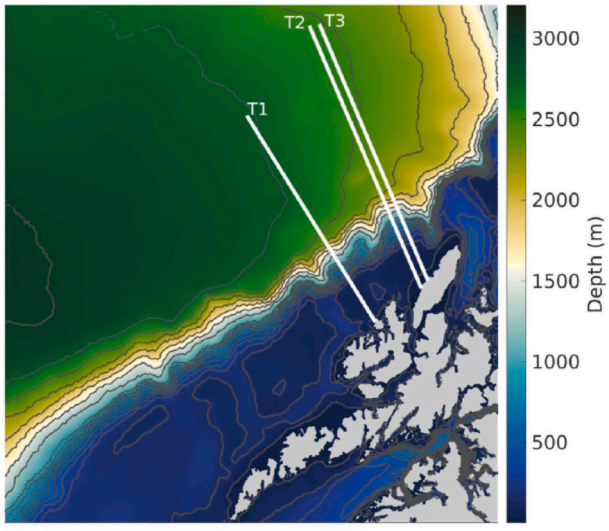

Fig. 2. Positions of transects T1, T2, T3 across the shelf outside Vesterålen.

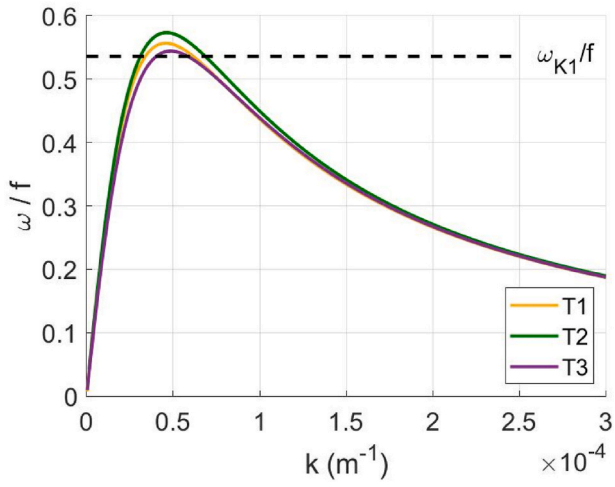

Fig. 3. Dispersion diagrams for transcects T1, T2, T3 outside Vesterålen (first mode), showing non-dimensional frequency ω/f *vs* wave number k. Here $f = 1.3\%10^{-4}\ s^{-1}$ is the Coriolis parameter. The upper horizontal dashed line is the non-dimensional tidal frequency for the K_1 component.

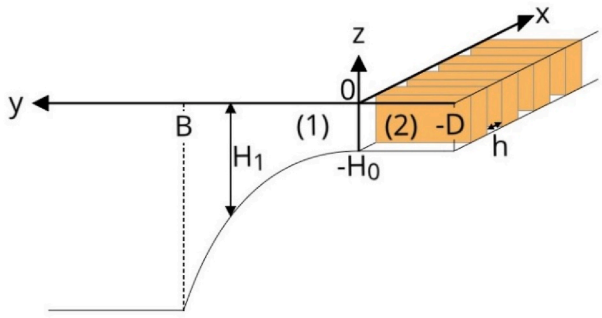

Fig. 4. A diagram showing the configuration with a coastal inner region $-D \leq y \leq 0$ of constant depth which is modelled by a series of Hele Shaw cells (vertical thin plates at a small distance h).

propagates along the shelf slope. We note that this phenomenon is a clear parallel to the damping of surface waves over a permeable seabed by Reid and Kajiura (1957); see also Webber and Huppert (2020) for surface waves over coral reefs.

We demonstrate that a non-zero velocity normal to the coastline inevitably will lead to a spatial damping of the CSWs. In a recent paper (Weber and Børve, 2021) this is done by applying a Robin condition (Gustafson, 1998) at the coastal boundary. The Robin condition is a weighted combination of Dirichlet boundary conditions and Neumann boundary conditions and is common in many branches of physics. The Robin condition, through a small parameter, allows for a small velocity normal to the coastline, which is exactly what happens when we have an inner shelf region with narrow fjords and small islands. The damping rate is then obtained as a function of the small Robin parameter.

In the present paper, we attempt to model the inner shelf near Lofoten-Vesterålen in north Norway in a less mathematical way. Since on average most of the narrow fjords are perpendicular to the coastline, we model them by a Hele Shaw geometry (Hele Shaw, 1898) with thin vertical plates normal to the coast; see also Batchelor (1967). Between two adjacent plates, we assume a balance between the pressure gradient force and an eddy viscous force. If the plates are sufficiently close, we can average the pressure-driven quadratic flow between them and obtain a mean friction force that is proportional to the (negative) mean velocity. In this way, the fjord system acts as a macroscopic porous medium, obeying Darcy's law (Bear, 1972) in the direction normal to the coast. By matching the mean velocity and the pressure at the boundary between the permeable inner shelf and the inviscid outer CSW region, we find the complex dispersion relation for the CSWs, yielding the spatial damping rate.

The rest of this paper is structured as follows: Section 2 presents the mathematical formulation of the flow on the outer and inner shelf. Section 3 yields the complex dispersion relation, while Section 4 discusses the mean drift in this case. Finally, Section 5 contains some concluding remarks.

2. Mathematical formulation

The shelf geometry with the trapped CSWs is adapted from Buchwald and Adams (1968). However, instead of assuming a solid or completely open boundary at the shelf break, we now formulate a boundary that is partly permeable. This is motivated by the fact that the western coast of Norway contains a myriad of narrow fjords and small islands through which the shelf water may percolate. In Fig. 4, we have depicted the geometry of our problem. The x axis is placed along the shelf break, and

the y axis is directed toward the sea. The z axis is vertically upwards. The velocity components in the various directions are (u,v,w), while the free surface is given by $z = \eta$. In our application to Lofoten-Vesterålen, the continental shelf is quite narrow, and the bottom profile is given by $z = -H(y)$ where

$$H = \begin{cases} H_0, & -D \le y \le 0 \\ H_0 \exp(2by), & 0 \le y \le B \\ H_0 \exp(2bB), & y \ge B. \end{cases} \tag{1}$$

Here b is a constant describing the steepness of the slope, and B is the width of the sloping shelf. One possible way to model the energy loss due narrow fjords and straits on the inner shelf, is to describe this region as consisting of a series of vertical Hele Shaw cells (Hele Shaw, 1898) at a small distance h; see Fig. 4.

2.1. The sloping shelf region

The linear CSW problem is solved along the lines of Buchwald and Adams (1968), and Gill and Schumann (1974); see also Gill (1982). Using mid-depth as a reference depth in the Lofoten area, the barotropic Rossby radius.

a_0 is of the order 900 km, while the shelf width B is typically 60 km. Hence, in the sloping shelf region (1), we have $B^2/a_0^2 \ll 1$. This means that we can make the rigid lid approximation (Gill and Schumann, 1974). In fact, a more thorough analysis for the CSW Eigen modes, allowing for a moving surface, shows that the rigid lid approximation is indeed well fulfilled for the Lofoten region; see (Drivdal et al., 2016, their Fig. 5).

The continuity equation then allows for the introduction of a stream function ψ_1 such that $u_1 H_1 = -\psi_{1y}$ and $v_1 H_1 = \psi_{1x}$, where subscripts denote partial derivatives. We assume that the waves are so long that the pressure is hydrostatic in the vertical direction. The following analysis is standard, and we just give a short outline. Neglecting any effects of friction in the shelf region (1), the linearized momentum equations become

$$-\psi_{1ty} - f\psi_{1x} = -gH_1\eta_{1x} \tag{2}$$

$$\psi_{1tx} - f\psi_{1y} = -gH_1\eta_{1y} \tag{3}$$

Here f is the constant Coriolis parameter, and g is the acceleration due to gravity. We now introduce a travelling wave solution (Gill, 1982) by

$$\psi_1 = H_1^{1/2}\varphi_1(y)\exp i(\kappa x - \omega t) \tag{4}$$

where κ is the complex wave number and ω is the real frequency. Then the governing equations reduce to

$$\varphi_1'' + l^2\varphi_1 = 0 \tag{5}$$

where the prime denotes derivation with respect to y, and

$$l^2 = 2fb\kappa/\omega - b^2 - \kappa^2 \tag{6}$$

At the edge of the shelf $y = B$, we must generally have continuity of pressure and normal fluxes. Utilizing that the deep ocean has a flat bottom, it is easy to show that the continuity conditions imply for the stream function at the shelf edge that

$$\psi_{1y} + \kappa\psi_1 = 0, \quad y = B. \tag{7}$$

(Weber and Drivdal, 2012). In terms of the φ_1 function, the boundary condition becomes

$$\varphi_1' + (b+\kappa)\varphi_1 = 0 \quad y = B \tag{8}$$

Writing the solution to (5) as

$$\varphi_1 = H_0^{-1/2}[A_1 \sin l(y-B) + C_1 \cos l(y-B)] \tag{9}$$

we find by applying (8) that $C_1 = -lA_1/(b+\kappa)$. Hence,

$$\varphi_1 = A_1 H_0^{-1/2}[\sin l(y-B) - (l/(b+\kappa))\cos l(y-B)] \tag{10}$$

We then obtain for the volume flux normal to the coast and the surface elevation

$$V_1 = Hv_1 = i\kappa H^{1/2}\varphi_1 \exp i(\kappa x - \omega t) \tag{11}$$

$$\eta_1 = (1/(gH^{1/2}\kappa))[(\kappa f - b\omega)\varphi_1 - \omega\varphi_1']\exp i(\kappa x - \omega t) \tag{12}$$

These quantities are needed for matching with the corresponding solutions on the inner shelf.

2.2. The permeable inner shelf

The reader is referred to Batchelor (1967) for a more thorough discussion of the Hele Shaw concept. The important point here is that the inner shelf region now becomes a sink of wave energy, so that the CSW, through exchange of water with the inner shelf, will suffer attenuation as it propagates along the contours of the sloping shelf.

If the horizontal distance h between the plates in Fig. 4 is sufficiently small, we can neglect the motion in the x direction. In each cell we assume a balance in the y-direction between the pressure gradient and the viscous force, leading to

$$0 = -\frac{1}{\rho}p_{2y} + \nu v_{2xx} \tag{13}$$

where ν is the kinematic eddy viscosity. In (13) we have assumed that $|v_{2xx}| \gg |v_{2yy}|, |v_{2zz}|$ since the separation between the plates is small. Furthermore, in each cell we assume hydrostatic balance in the vertical, that is

$$p_2 = -\rho g(z - \eta_2) \tag{14}$$

where η_2 is the surface elevation. From (13) and (14), assuming no-slip at $x = 0, h$, we obtain a velocity which is quadratic in x. Averaging between the planes, the oscillatory velocity can be written

$$\overline{v}_2 = \frac{1}{h}\int_0^h v_2 dx = -[gh^2/(12\nu)]\overline{\eta}_{2y} \tag{15}$$

By rearranging, we arrive at

$$0 = -g\overline{\eta}_{2y} - (\nu/K)\overline{v}_2 \tag{16}$$

We realize that (16) expresses Darcy's law for a porous medium (Bear, 1972), where $K = h^2/12$ is the effective permeability.

The continuity equation in the Hele Shaw cell becomes

$$\overline{v}_{2y} + \overline{w}_{2z} = 0 \tag{17}$$

By integrating (17) in the vertical, we obtain

$$\overline{\eta}_{2t} = -H_0\overline{v}_{2y} \tag{18}$$

Insertion into (16), and assuming $\overline{v}_2 \propto \exp i(\kappa x - \omega t)$, we find

$$\overline{v}_{2yy} - \gamma^2\overline{v}_2 = 0 \tag{19}$$

where

$$\gamma^2 = -i\omega\nu/(gH_0K) \tag{20}$$

We assume that the onshore velocity vanishes at the end of the permeable shelf region (2), i.e.

$\overline{v}_2(y = -D) = 0$. The solutions then become

$$\overline{V}_2 = H_0\overline{v}_2 = A_2H_0 \sinh\gamma(y+D)\exp i(\kappa x - \omega t) \tag{21}$$

$$\overline{\eta}_2 = -(i\gamma H_0/\omega)A_2 \cosh\gamma(y+D)\exp i(\kappa x - \omega t) \tag{22}$$

where the constant A_2 is related to the shelf wave constant A_1 in (10) through the matching conditions.

3. Matching conditions and the dispersion relation

At the shelf break, the volume flux normal to the coastline and the surface elevation (i.e. pressure) must be continuous. Hence, since $H_1(0) = H_0$,

$$v_1 = \overline{v}_2 \quad y = 0, \tag{23}$$

$$\eta_1 = \overline{\eta}_2 \quad y = 0, \tag{24}$$

Inserting from (11) and (21) into (23), we obtain

$$A_2 = -(i\kappa / (H_0 \sinh \gamma D))[\sin lB + (l/(b+\kappa))\cos lB]A_1 \tag{25}$$

Finally, utilizing (25), we find from (12), (22) and (24) the complex dispersion relation for this problem:

$$\tan lB + l/(b+\kappa) = -[\omega^2 \tanh \gamma D / (2\gamma g H_0 \kappa^2 b(b+\kappa))](Q_1 \tan lB - Q_2) \tag{26}$$

where

$$Q_1 = b^3 + bl^2 + \kappa(b^2 - l^2 - b\kappa - \kappa^2) \tag{27}$$

and

$$Q_2 = l(b+\kappa)^2 + l^3 \tag{28}$$

In (26), κ, l, γ are complex quantities. From the definition (20), we find

$$\gamma = (1-i)\omega(2gH_0)^{-1/2}R^{-1/2} \tag{29}$$

where we have defined a small parameter R by

$$R = \omega K/\nu \tag{30}$$

For surface waves over a porous bed, Reid and Kajiura (1957) find that R is a fundamental small parameter of the porous problem. We assume that this is also the case for our permeable shelf. Then we realize that γD in (26) is a large dimensionless quantity. Accordingly, we have that $\tanh \gamma D \sim 1$. Hence, we may write (26) as

$$\tan lB + l/(b+\kappa) = -(1+i)\omega(Q_1 \tan lB - Q_2)R^{1/2} / [2(2gH_0)^{1/2}\kappa^2 b(b+\kappa)] \tag{31}$$

In this paper, we consider spatial damping:

$$\kappa = k + i\alpha \tag{32}$$

where the real part of the wave number k is the free variable in this problem. We assume that the imaginary part α (the spatial damping rate) is a small quantity. Since ω is real, it follows from (6) that l is complex. We take

$$l = l_0 + i\delta \tag{33}$$

where $\delta \sim O(\alpha)$. The lowest order solution of (31) yields $l_0 = l_0(k)$. We assume that the modified frequency is $\omega = \omega_0 + O(\alpha/k)^2$. Then, from the real part of (6) to lowest order

$$\omega_0 = 2fbk/(b^2 + l_0^2 + k^2) \tag{34}$$

For the imaginary part to $O(\alpha)$ we obtain

$$\delta = (\alpha/k)[b^2 + l_0^2 - k^2]/(2l_0) \tag{35}$$

Inserting into (6), we find that $\omega = \omega_0 + O(\alpha^2/k^2)$ as anticipated. What now remains is to determine l_0 and α from the real and imaginary parts of (31).

Using (32)-(33), and expanding the trigonometric functions appearing in (31), we find from the real part to lowest order that

$$\tan l_0 B = -l_0/(b+k) \tag{36}$$

as in Buchwald and Adams (1968).

From the imaginary part, using (35), we obtain to $O(\alpha/k)$ that

$$\alpha = c(gH_0)^{-1/2} l_0^2[(b+k)^2 + l_0^2](2R)^{1/2}/M \tag{37}$$

where $c = \omega_0/k$ is the phase speed. Furthermore, we have defined

$$M = (b^2 + l_0^2 - k^2)(b + k + B(b+k)^2 + Bl_0^2) - 2kl_0^2 \tag{38}$$

At this point, it is convenient to introduce the group velocity $c_g = \partial \omega_0/\partial k$ into the problem. From Weber and Drivdal (2012) we obtain, when using (38):

$$c_g = cM / [(b^2 + l_0^2 + k^2)(b + k + B(b+k)^2 + Bl_0^2)] \tag{39}$$

Inserting for M, we can write the dimensionless spatial damping rate (37) as

$$\alpha/k = Nc^2(gH_0)^{-1/2}(2R)^{1/2}/c_g \tag{40}$$

Here N is a positive dimensionless quantity defined by

$$N = k^{-1}l_0^2((b+k)^2 + l_0^2) / [(b^2 + l_0^2 + k^2)(b + k + B(b+k)^2 + Bl_0^2)] \tag{41}$$

We notice that α/k in (40) becomes infinitely large when $c_g \to 0$. It is positive when approached from the smaller wave number side and negative when approached from the larger wave number side. In the latter case it must be remembered that $x < 0$, so $\alpha x > 0$ in the attenuation factor $\exp(-\alpha x)$. Obviously, our calculations assuming a small damping rate is not valid here, but this singular behavior indicates that no wave energy escapes in either direction from the point where the group velocity is zero.

From a barotropic numerical model for tidal motion, Børve et al. (2021) compute a distinct amplification of the current speed in the Lofoten region for the diurnal K_1 tidal component. This amplification was also observed by Moe et al. (2002), and model calculations in the same study imply the existence of short CSWs on the shelf outside Lofoten with diurnal frequency. These findings support the theoretical behavior predicted in the present paper of an energy accumulation at the K_1 frequency in a region where the group velocity is nearly zero.

In Weber and Børve (2021), the spatial damping of the wave field is obtained by applying a Robin condition (Gustafson, 1998) at the permeable coastal boundary. In the present notation, the Robin condition can be written as

$$rv_{1y} + v_1 = 0, \quad y = 0, \tag{42}$$

where r is the small Robin parameter. With this condition, the spatial damping rate becomes (Weber and Børve, 2021)

$$\alpha/k = [2Bl_0^2\{(b+k)^2 + l_0^2\} / \{(b^2 + l_0^2 + k^2)L\}](c/c_g)(r/B) \tag{43}$$

Here

$$L = b + k + B(b+k)^2 + Bl_0^2 \tag{44}$$

By comparing (40) and (43), we can express the Robin parameter in terms of the physical parameters (permeability, eddy viscosity) that characterize the flow on the inner porous shelf. We then find for the dimensionless Robin parameter

$$rk = [c/(2gH_0)^{1/2}](\omega K/\nu)^{1/2} \tag{45}$$

4. The mean drift over the shelf

Weber and Børve (2021) present an analysis of the non-linear mean drift currents due to spatially damped diurnal CSWs. The fluid over the shelf is assumed to be inviscid, and the damping occurs through a small exchange of fluid through the coastal boundary. The Lagrangian mean drift current is found to be independent of the value of the small Robin parameter rk, as long as it is non-zero.

The dynamical problem in Weber and Børve (2021) is similar to the present one with a porous inner shelf. For the same geometry, the wave solutions over the shelf become equal. The expressions for the damping coefficient and the imaginary part of the cross-shelf wave number δ are different in the two cases, but the relation between them, i.e. eqn. (35), is the same. As a result, the calculation of the radiation stresses that drive the Lagrangian mean currents is the same in the two cases. This means that the spatial mean current distribution over the sloping shelf becomes unaltered when we compare the Robin case and the porous inner shelf case.

As a reminder of the importance this drift current potentially has for the transport cod egg and larvae from the spawning sites in the Lofoten-Vesterålen region, we make a brief revisit. In Fig. 5 we have plotted the Lagrangian (particle-following) mean non-dimensional velocity $\overline{u}_L/\ u_0$ over an idealized Vesterålen shelf (1), where $H_0 = 50$ m, $B = 60$ km and $b = 3.2\%10^{-5}\ \mathrm{m}^{-1}$. Furthermore, from Fig. 3, the diurnal CSW with positive group velocity has an along-shore wave number $k = 4\%10^{-5}\mathrm{m}^{-1}$. From (36) we find $l_0 = 4.3\%10^{-5}\ \mathrm{m}^{-1}$ for the corresponding cross-shore wave number (first mode). For details concerning the calculation of the non-linear current, we refer to Weber and Børve (2021).

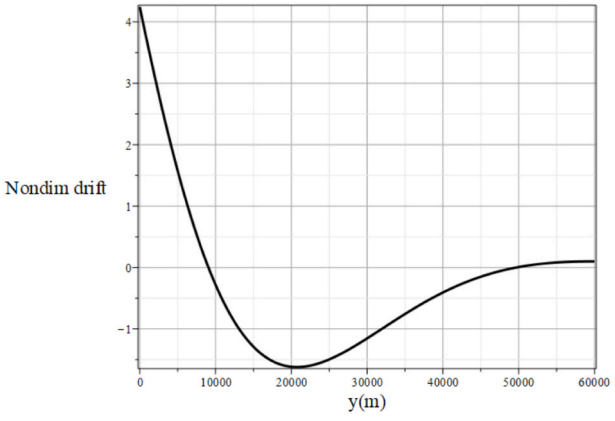

Fig. 5. The non-dimensional Lagrangian drift velocity $\overline{u}_L/\ u_0$ over the sloping shelf (1) as function of the seaward coordinate. The velocity scale is $u_0 = A_1^2 b^3 \exp(-2\alpha x)/(fH_0^2)$, where A_1 is the shelf wave constant in (10), and α is the attenuation rate (40) for the case of a porous inner shelf.

We observe from the figure that the Lagrangian drift velocity is basically located over the shallow part of the shelf with a positive (northward) value at the inner 10 km, and a distinct maximum at the coast. Between 10 km and 50 km the drift is negative (southward) with a smaller maximum value.

5. Concluding remarks

The spatial damping coefficient for a CSW on a shelf where the inner archipelago is modelled as a porous medium, is proportional to the inverse group velocity. Hence, in the case where the local group velocity tends to zero, there will be an accumulation of wave energy in this region. This may occur for CSWs with the diurnal K_1 tidal frequency in the Lofoten-Vesterålen region in north Norway. For the mean drift currents induced by the CSWs, it is interesting to note that the actual modelling of the permeable coastal boundary that separates the inner archipelago from the sloping outer shelf (Robin/Hele Shaw) is not crucial. The important point is that the coastal boundary must allow for a small non-zero velocity normal to the coast. This induces the small spatial damping of the linear wave field, which in turn determines the driving forces for the nonlinear Lagrangian drift current.

Declaration of competing interest

The authors declare that they have no known competing financial interests or personal relationships that could have appeared to influence the work reported in this paper.

Acknowledgements

The authors gratefully acknowledge support from the Research Council of Norway through Grant 280625 (JEW, travel) and by VISTA – a basic research program in collaboration between The Norwegian Academy of Science and Letters, and Equinor (EB, funding). The bathymetry data used in Fig. 1 is attributed GEBCO Compilation Group (2021) GEBCO 2021 Grid (https://doi.org/10.5285/c6612cbe-50b3-0cff-e053-6c86abc09f8f). The bottom topography in Fig. 2 is provided by the Norwegian Mapping Authority. The authors gratefully thank the group for releasing the data for public access.

References

Batchelor, G.K., 1967. An Introduction to Fluid Dynamics. Cambridge University Press, p. 615.
Bear, J., 1972. Dynamics of Fluids in Porous Media. American Elsevier Publ. Comp, p. 764.
Buchwald, V.T., Adams, J.K., 1968. The propagation of continental shelf waves. Proc. Roy. Soc. Lond. 305, 235–250.
Buchwald, V.T., Kachoyan, B.J., 1987. Shelf waves generated by coastal flux. Aust. J. Mar. Freshw. Res. 38, 429–437.
Børve, E., Isachsen, P.E., Nøst, O.A., 2021. Rectified tidal transport in Lofoten-Vesterålen, Northern Norway. Ocean Sci. 17, 1753–1773. https://doi.org/10.5194/os-17-1753-2021.
Cartwright, D.E., 1969. Extraordinary tidal currents near St. Kilda. Nature 223, 928–993.
Drivdal, M., Weber, J.E., Debernard, J.B., 2016. Dispersion relation for continental shelf waves when the shallow shelf part has an arbitrary width: application to the shelf west of Norway. J. Phys. Oceanogr. 46, 537–549.
Foreman, M.G.G., Thomson, R.E., 1997. Three-dimensional model simulations of tides and buoyancy currents along the west coast of Vancouver island. J. Phys. Oceanogr. 27, 1300–1325.
Gill, A.E., 1982. Atmosphere-ocean dynamics. In: Int. Geophys. Ser., 30. Academic Press, p. 662.
Gill, A.E., Schumann, E.H., 1974. The generation of long shelf waves by the wind. J. Phys. Oceanogr. 4, 83–90.
Gustafson, K., 1998. Domain decomposition, operator trigonometry, Robin condition. Contemp. Math. 218, 432–437.

Hele Shaw, H.J.S., 1898. The flow of water. Nature 58, 34–36.
Lam, F.-P.A., 1999. Shelf waves with diurnal tidal frequency at the Greenland shelf edge. Deep-Sea Res. I 46, 895–923.
Middleton, J.F., 1988. Long shelf waves generated by a coastal flux. J. Geophys. Res. 93 (10), 724-10,730.
Moe, H., Ommundsen, A., Gjevik, B., 2002. A high resolution tidal model for the area around. The Lofoten Islands. Continent. Shelf Res. 22, 485–504.
Morrow, R.A., Jones, I.S.F., Smith, R.L., Stabeno, P.J., 1990. Bass Strait forcing of coastal trapped waves: ACE revisited. J. Phys. Oceanogr. 20, 1528–1538.
Ommundsen, A., Gjevik, B., 2000. Scattering of Tidal Kelvin Waves along Shelves Which Varyin Their Lengthwise Direction. Preprint Series, Department of Mathematics, University of Oslo, p. 24.
Reid, R.O., Kajiura, K., 1957. On the damping of gravity waves over a permeable sea bed. Trans. Am. Geophys. Union 38, 662–666.
Webber, J.J., Huppert, H.E., 2020. Stokes drift in coral reefs with depth-varying permeability. Phil. Trans. R. Soc. A 378, 20190531.
Weber, J.E., Drivdal, M., 2012. Radiation stress and mean drift in continental shelf waves. Continent. Shelf Res. 35, 108–116.
Weber, J.E., Børve, E., 2021. Diurnal continental shelf waves with a permeable coastal boundary: application to the shelf northwest of Norway. European J. Mech. / B Fluids 86, 64–71.